



1 in Salinas, CA during the winter months of 2013/14 and 2014/15 using rotating arm impaction  
2 spore trap samplers coupled with quantitative PCR (qPCR). Low levels of *P. effusa* DNA were  
3 detectable from December through February in both seasons, but increased during January in  
4 both years, in correlation with observed disease incidence; sharp peaks in *P. effusa* DNA  
5 detection were associated with the onset of disease incidence. Disease incidence ratings in the  
6 susceptible field suggested that spinach downy mildew displays logistic dynamics but with  
7 considerable inter-season variation; the epidemic in 2014 was more severe than in 2015. Spatial  
8 analyses indicated that disease incidence is spatially dependent within an average range of 5.9 m,  
9 approximately equivalent to the width of three planted beds in a typical production field. The  
10 spatial distribution of spores captured during an active epidemic could be fit with either the  
11 power-law or exponential distributions. These findings revealed the utility of impaction spore  
12 trap samplers linked with a qPCR assay for indicating periods of high disease risk, long distance  
13 dispersal of *P. effusa* spores, and the spatial aggregation of disease incidence.

14

---

15 Spinach is an economically important leafy green vegetable and has been increasingly  
16 consumed as an important part of a healthy diet (Correll et al. 2011). Increasing demand for  
17 fresh market spinach has driven changes in production in the US, such as the use of wider beds  
18 and denser plantings (Koike et al. 2011). In the US, most spring and summer spinach production  
19 occurs in the Salinas Valley of California, whereas fall and winter production occurs in the  
20 Imperial and Yuma valleys of California and Arizona, respectively. Together these regions  
21 account for over 90% of the spinach produced in the US annually (USDA-NASS 2015). The  
22 seasonal shift in production is driven by the optimal growth conditions of spinach and the year-  
23 long demand for fresh market spinach. There is little to no commercial fresh market spinach

1 production in these regions during their respective off-seasons. In all regions where spinach is  
2 grown, increasing production has coincided with an increase in downy mildew (Correll et al.,  
3 2011).

4 Downy mildew is a threat to spinach worldwide (Correll et al., 2011) and is caused by the  
5 obligate oomycete biotroph *Peronospora effusa* (Grev.) Rabenh (previously *P. farinosa* f. sp.  
6 *spinaciae*) (Choi et al. 2007; Thines and Choi 2016). *Peronospora effusa* is endemic to all  
7 spinach growing regions, and co-occurs with many other closely related downy mildew species  
8 (Choi et al. 2007; Klosterman et al. 2014). *Peronospora effusa* proliferates in cool, moist  
9 conditions, and can spread rapidly through the production of airborne sporangia (Frinking and  
10 van der Stoel 1987). Downy mildew causes chlorosis of spinach leaves and plant decline,  
11 reducing acceptability of the fresh market crop to packers and shippers. In recent years, a series  
12 of new pathogen races has overcome several resistant varieties, leading to increased crop losses,  
13 especially for organic growers who cannot use synthetic pesticides for disease control (Feng et  
14 al. 2014). Recent work has focused on monitoring airborne populations of *P. effusa* during the  
15 main growing season in the Salinas Valley using a qPCR assay linked with an impaction spore  
16 trap sampler (Klosterman et al. 2014). This work discovered an overall exponential increase in  
17 the *P. effusa* levels over the course of the season in the Salinas Valley, as well as detecting *P.*  
18 *effusa* even in the early portion of the growing season (Choudhury et al., unpublished).

19 Little is known about how airborne inoculum levels of *P. effusa* fluctuate during the off-  
20 season in the Salinas Valley, when spinach is only planted sparingly for processing. All obligate  
21 biotrophic pathogens need to survive host-free periods that often occur during winter in  
22 temperate climates. Overwintering strategies differ between obligate pathogens; some produce  
23 durable, dormant structures and others rely on green bridge crops to propagate and survive

1 (Gadoury et al. 2012; McDonald and Linde 2002; Montarry et al. 2007; Spanu 2012). These  
2 strategies are often dependent on the host and local agronomic practices, which may limit  
3 success.

4 Cross-inoculation studies suggest that *P. effusa* only affects spinach plants and cannot infect  
5 other closely related cultivated plants such as beets and Swiss chard (Byford 1967; Klosterman et  
6 al. 2014). Phylogenetic analyses indicate that *P. effusa* is distinct from other *Peronospora* spp.  
7 (Choi et al. 2015). This host specificity would limit the ability of *P. effusa* to overwinter by  
8 reducing the number of viable hosts. While it is difficult to fully exclude the possibility of  
9 infection on volunteer spinach plants, the relatively rapid progression of disease symptoms from  
10 infection to sporulation and decline suggests that this is unlikely (van den Bosch et al. 1988).  
11 Understanding how over-wintering populations survive and fluctuate in levels may lead to more  
12 effective disease control strategies.

13 Without suitable alternative hosts in the absence of spinach crops, spinach downy mildew  
14 populations are thought to decline. In other downy mildew systems, these host-free periods are  
15 sometimes characterized by local extirpation and recolonization events (LaMondia and Aylor  
16 2001). Recolonization events can be mediated by asymptomatic infection of transplant  
17 seedlings, germination and infection of soil- or seed-borne oospores, movement of pathogen  
18 propagules on infested farm equipment, or long distance dispersal (LDD) of airborne spores  
19 (Aylor 2003; Ojiambo and Holmes 2011). These LDD events have been hypothesized as the  
20 cause of disease outbreaks for several plant pathogens, as well as the possible inter-continental  
21 introduction of new pathogens (Aylor 2003; Brown and Hovmøller 2001). Environmental  
22 microbiologists also observed long distance deposition of microbes and particulates at  
23 continental scales (Kellogg and Griffin 2006). Dispersal events of plant pathogens often take

1 place at multiple scales, expanding outwards through the creation of new disease foci (Zadoks  
2 and van den Bosch 1994). As disease foci converge, the emerging disease front appears as an  
3 expanding wave on the landscape. Understanding how regional spore dispersal impacts disease  
4 is critical for proper disease control. Monitoring airborne *P. effusa* levels during the off-season  
5 may reveal cryptic features of the pathogen's life cycle that may explain its capacity for rapid  
6 population increase during the host growing season.

7 While several studies have shown how rapidly other closely related downy mildew species  
8 colonize and spread (Ojiambo and Holmes 2011; Stein et al. 1994; Wu et al. 2001), there are  
9 relatively little data on the spatio-temporal patterns of spinach downy mildew. This is especially  
10 true in regards to the situation with more modern production practices, such as denser spinach  
11 plantings in wider beds, and increasing acreage of production (Koike et al. 2011). Without this  
12 information, it is difficult to predict how a single diseased field might affect disease within a  
13 region.

14 In this study, we used impaction spore trap samplers and qPCR assays to monitor airborne *P.*  
15 *effusa* levels over two winter periods in the Salinas Valley. We also monitored the progress of  
16 disease incidence in nearby fields of susceptible spinach. The study had three goals: (1) to  
17 understand how airborne *P. effusa* levels vary over the winter months, when relatively little  
18 commercial spinach is grown; (2) to characterize the spatio-temporal patterns of disease  
19 progression; and (3) to understand long distance dispersal patterns of *P. effusa* spores.

20

21

## MATERIALS AND METHODS

22

23

Field Site: Four 2-m beds (approximately 37 m × 10 m) of spinach cultivar 'Viroflay' were  
planted at the Hartnell College East Campus site in Salinas, CA on November 25, 2013 and

1 maintained until February 11, 2014. The same site was planted again with Viroflay on  
2 November 20, 2014 and maintained until February 6, 2015. ‘Viroflay’ is universally susceptible  
3 to all races of spinach downy mildew (Feng et al. 2014). The field sites were planted at a density  
4 of 5 million seeds per hectare. The sites were supplied with supplemental overhead irrigation  
5 twice each week in the absence of rain, mimicking conditions used by commercial growers.

6 Disease incidence rating: Disease incidence ratings at the Salinas 2013-2014 and Salinas  
7 2014-2015 sites were conducted on a weekly basis beginning when plants had four true leaves.  
8 One square meter areas were marked out with flags on every row, spaced evenly apart every 4  
9 meters. These disease incidence blocks were rated for presence or absence of downy mildew  
10 symptoms on individual leaves, and ratings were expressed as the proportion of disease leaves in  
11 the rated area. In Salinas 2014-2015, two adjacent disease incidence blocks were used per row.

12 Spore trapping and qPCR: Rotating arm impaction spore trap samplers (Fallacy et al. 2007;  
13 Thiessen et al. 2016) were placed approximately 2 m from the edge at the four cardinal points  
14 around the susceptible spinach field in the Salinas 2013-2014 and Salinas 2014-2015 seasons.  
15 The 40 mm stainless steel, grease-coated spore trap rods (316LSi stainless steel; Harris Products  
16 Group, Mason, OH) were collected three times a week from late-November to mid-February in  
17 both years. The rods were stored at 4°C for 1 to 2 weeks until DNA extractions were performed.  
18 Remaining extracted samples were stored at -80°C.

19 DNA extractions from rods were carried out using a NucleoSpin® Plant II kit (Machery-  
20 Nagel). The qPCR (TaqMan) assays were conducted with the SNP-specific primers for *P. effusa*  
21 and *P. schachtii*, and results were expressed as copy number of *P. effusa* ribosomal DNA as  
22 previously described (Klosterman et al. 2014).

1        Long distance distribution: As reported previously (Klosterman et al. 2014), two spore traps  
2 were placed next to a commercial spinach field in Soledad, CA that had an active downy mildew  
3 outbreak during March 13 to April 3, 2013. One spore trap was placed at the north end and one  
4 approximately 750 m apart at the south end of this spinach field. The other site examined for  
5 long distance distribution was the Salinas 2013-2014 site (described above under field site).  
6 Spore trapping at Soledad 2013 and the Salinas 2013-2014 epidemic was concurrent with other  
7 spore trap samplings throughout the Salinas Valley, at four other locations roughly 15 to 20 km  
8 apart. For all trap sites, the spore trap rods were collected three times per week. The Salinas  
9 2014-2015 field site was not included because there were no other trapping efforts in the Salinas  
10 Valley during that period.

11        Weather data: High quality weather data for individual sites were generated by Fox Weather,  
12 LLC using the MtnRT® custom software described by Fox (2011). For the basic initial data, we  
13 used the North American Regional Reanalysis (NARR), obtained from NOAA at 32 km  
14 gridspacing and 3 hour time step. From the NARR data, we produced sequential nested WRF  
15 runs (4 km grid) to provide input for MtnRT. Using MtnRT, running at a 1.5 km grid, we  
16 produced a continuous record of hourly data, including wind direction and speed at 2 m and 50 m  
17 above ground, and the other weather parameters mentioned above. The forecast point locations  
18 for the two winter periods included the following stations: 201 at 36.6245N, 121.5393W, and  
19 206 at 36.6701N, 121.6047W. For February 2015, the NARR data were not available.  
20 Therefore the WRF 12 km was used with forecast hours t+6 to t+24 from Fox Weather's  
21 operational WRF archive to produce data for the MtnRT simulations.

22        The MtnRT processing included the interpolation to 1 hour increments for the surface  
23 weather data, including wind direction and speed (Mesinger et al. 2006). This included

1 consideration of MtnRT's calculation of wind vector variations resulting from development of  
2 nocturnal inversions. Wind speed was calculated at 2 m height above ground instead of the  
3 standard 10 m height. This was done to better represent wind speeds at top of the canopy for  
4 spinach or lettuce crops. The calculation of wind speed at 2 m was based on a logarithmic  
5 relationship of wind speed versus distance above ground. A simplified version of the theoretical  
6 logarithmic relationship is  $U_2 = U_1 (\ln (h_2/z_0)/\ln (h_1/z_0))$ , where  $U_2$  is wind speed to be  
7 calculated (in this case at  $h_2=2$  m), while  $U_1$  is the speed at the reference height  $h_1$ ). The value  
8 of roughness length  $z_0$  for most purposes would be 0.1 to 0.2 for the environment that includes  
9 the field plot. For illustration, given a reference height of 50 m and speed  $U_1$  of 10 m/s, the 2 m  
10 speed  $U_2$  would be close to 3 m/s, and 10 m speed 4.1 m/s.

11 When necessary, supplemental weather data for the Salinas 2013-2014 and Salinas 2014-  
12 2015 seasons were collected from the nearby Salinas CIMIS weather station (Salinas South II,  
13 Station #214) and the Salinas Municipal Airport weather station (KSNS). Weather data collected  
14 from the CIMIS station included hourly measurements of temperature, relative humidity, wind  
15 speed, and wind direction, and data collected from the airport station included hourly  
16 measurements of cloud coverage.

17 Analysis: Cluster analysis of spore trap temporal pattern similarity: The Euclidian distances  
18 between the temporal sequences of copy numbers from the four spore traps from the Salinas  
19 2013-2014 and Salinas 2014-2015 seasons were calculated using the standard distance  
20 equation:  $d(x, y) = \sqrt{\sum_{i=1}^n (x_i - y_i)^2}$ , where  $d$  is the distance (i.e. difference) between two spore  
21 copy number measurements  $x$  and  $y$ , and  $n$  is the number of measurements. Dendrograms of the  
22 hierarchical relationship between the spore traps were constructed using the unweighted pair  
23 group with arithmetic means method.

1     Temporal analysis: Disease progression over time at the Salinas 2013-2014 and Salinas  
 2 2014-2015 sites was examined by modeling disease incidence data with a nonlinear regression to  
 3 estimate the parameters of a logistic growth function. The standard logistic is defined by the  
 4 equation  $Y = \frac{K}{[1 + \beta^{(-rt)}]}$  with  $Y$  and  $t$  representing the percent disease incidence and the number  
 5 of days after the first disease rating, respectively. The coefficients  $K$ ,  $r$ , and  $\beta$  are the maximum  
 6 disease level, the rate parameter, and the constant term (capturing the initial condition) of the  
 7 model, respectively. The rate of change of disease level  $Y$  at time  $t$  was determined using the  
 8 derivative  $Y'(t) = rY(K - Y)$ . The area under the disease progress curve (AUDPC) was  
 9 calculated for the epidemics in 2014 and 2015. The area approximates the amount of disease in a  
 10 given season, and is commonly used to compare epidemics from different regions or time spans  
 11 (Madden et al. 2007).

12     Spatial-analysis of disease incidence data: Spatial correlations between disease incidence  
 13 blocks at the Salinas 2013-2014 and Salinas 2014-2015 sites were determined by analyzing  
 14 isotropic semivariograms. Semivariograms measure the average variability between the points  $z_i$   
 15 and  $z_{i+h}$  lying  $h$  distance apart inside of the field plot (Mouen Bedimo et al., 2007). Statistically,  
 16 semivariance is related to the autocorrelation and is defined by the function  $\gamma(h) =$   
 17  $[\frac{1}{2}n(h)] \sum [z_i - z_{i+h}]^2$ , where  $\gamma(h)$ , the semivariance for interval distance class  $h$ , is half the  
 18 average of the sum of square differences between the percentage of disease for  $n$  sample pairs of  
 19 disease incidence blocks, with lag interval  $h$ ;  $z_i$  is the disease incidence percent in the disease  
 20 blocks at point  $i$ , and  $z_{i+h}$  is the percentage measured for sample disease blocks at point  $i+h$ . The  
 21 data were fitted to the exponential, spherical, and Gaussian isotropic model variograms to  
 22 analyze the multidirectional spatial dependence between disease incidence blocks. All three  
 23 models are described by the range, the nugget, and the sill.

1       The range is the separation distance over which the samples are spatially dependent, the  
2 nugget ( $C_0$ ) is the y-intercept of the model, essentially the variance in disease incidence at zero  
3 lag (which may indicate errors in measurements or spatial dependence below the measured  
4 distance), and the sill ( $C + C_0$ ) is the asymptote of the model. The maximum log-composite-  
5 likelihood (MLCL) value, the residual sum of squares, the  $R^2$  coefficient, and the proportion of  
6  $C/(C_0 + C)$  are statistics that are often used to interpret the validity of the variogram models. The  
7 MLCL provides a measure of how well the model fits the variogram data, and is fairly robust in  
8 regards to assumptions of distributions and is computationally simple (Curriero and Lele 1999),  
9 providing advantages over similar methods, such as maximum likelihood and restricted  
10 maximum likelihood. The  $R^2$  coefficient provides an indication of how well the model fits the  
11 variogram data. The proportion of  $C/(C_0 + C)$  provides a measure of the proportion of the sill  
12 that is explained by spatially structured variance ( $C$ ). The proportion of  $C/(C_0 + C)$  will be 1 for  
13 a variogram with no nugget effect, and it will be 0 where there is no detectable spatial  
14 dependence at the range specified.

15       Distribution fitting to examine spore dispersal data: *Peronospora effusa* rDNA levels from  
16 the Soledad 2013 commercial field site and the Salinas 2013-2014 site were fitted to the power-  
17 law and exponential distributions as suggested by Clauset et al. (2009). The continuous power-  
18 law distribution is defined as  $f(x) = x^{-\alpha}$  where  $x$  is the quantity whose distribution we are  
19 interested in, and  $\alpha$  is the exponent or scaling parameter. Very few empirical data sets can fit a  
20 power law distribution for all  $x$  values; oftentimes, power-law (and other distributions) only  
21 apply for  $x$  values greater than some minimum, referred to as  $x_{min}$ . An appropriate  $x_{min}$  value was  
22 estimated by calculating the minimum  $x$  value that provided the lowest Kolmogorov–Smirnov  
23 (KS) statistic between the empirical and theoretical cumulative distribution function. An

1 appropriate  $\alpha$  value was then estimated using the maximum likelihood estimator equation:  $\hat{\alpha} =$   
2  $(1 + n) / \sum_{i=1}^n \ln(\frac{x_i}{x_{min}})$ . The continuous exponential distribution is defined as  $f(x) = e^{-\lambda x}$ ,  
3 where  $e$  is Euler's number (approximately 2.718) and  $\lambda$  is the exponential coefficient.  $\lambda$  was  
4 calculated using the equation  $\lambda = 1/(\bar{x} - x_{min})$ , where  $\bar{x}$  is the average of the *P. effusa* copy  
5 numbers and  $x_{min}$  is exponential distribution appropriate minimum value. After finding  
6 appropriate  $\alpha$ ,  $\lambda$ , and  $x_{min}$  values, the epidemic datasets were tested for the goodness of fit of their  
7 distribution against 2500 randomly generated datasets with the same parameters using the KS  
8 test.

9 The natural log of the *P. effusa* copy numbers was plotted against both the natural log of the  
10 distance and the untransformed distance from the outbreak. A small constant (1) was added to  
11 the distance data before natural log transformation to prevent undefined results. These data were  
12 fitted using a linear regression, as recommended by Fitt et al. (1987).

13

14

## RESULTS

15 Spore trapping: While *P. effusa* was detected in both Salinas 2013-2014 and Salinas 2014-  
16 2015 winter seasons, *P. effusa* levels increased dramatically over the course of both seasons (Fig.  
17 1). *P. effusa* levels increased steadily throughout the Salinas 2013-2014 season, and peaked as  
18 disease incidence levels began to rise. Detectable *Peronospora effusa* DNA levels in Salinas  
19 2014-2015 season increased rapidly through the winter season; late in the Salinas 2014-2015  
20 season detection of *P. effusa* was intermittent but increasing (Fig. 1), especially after mid-  
21 January at the Salinas site when the disease in the field was detected in both the 2013-2014 and  
22 2014-2015 seasons. Hierarchical clustering of the spore traps grouped the north and east traps  
23 and the south and west traps in both years (Fig. 2). The predominant wind directions occurring

1 at the site were bimodal, and came from the NW and SE in both the Salinas 2013-2014 and  
2 2014-2015 seasons (Fig. 3). The wind distribution impacted the observations of *P. effusa* DNA  
3 detection in both years, as detectable levels were observed on each of the four traps at the Salinas  
4 site in the 2013-2014 and 2014-2015 seasons, although the recorded levels did fluctuate between  
5 the four different traps (Figs. S1 and S2). Levels of *P. effusa* DNA were particularly higher in  
6 2013-2014 on the S and E traps in mid-January onward (Fig. S1), consistent with a NW wind  
7 flow. In the 2014-2015 season, detection was not concentrated at the South and East spore traps  
8 (Fig. S2), although the NW wind speeds were only slightly less in the 2014-2015 season (Fig. 3).

9 Disease incidence: Downy mildew symptoms were observed on spinach leaves for both  
10 winter seasons in the Salinas 2013-2014 and Salinas 2014-2015 plots (Fig. 1). Although the  
11 symptoms tended to occur in clusters, the entire field was quickly colonized in both seasons (Fig.  
12 1). Chlorotic symptoms on the leaves were often accompanied by sporulation, which most often  
13 occurred within the canopy of the spinach row.

14 Temporal analysis: Mean disease incidence had a close fit to a logistic curve for both the  
15 Salinas 2013-2014 and 2014-2015 seasons (Fig. 1, Table 1). The AUDPC of the 2013-2014 and  
16 2014-2015 epidemics were 3019.3 and 1282.9, respectively, indicating that the 2014-2015  
17 epidemic was much less severe, overall (Table 1). This difference in overall incidence is  
18 corroborated by the rate parameter ( $r$ ) and the final carrying capacity ( $K$ ), which indicate a more  
19 rapid and severe epidemic in the Salinas 2013-2014 season.

20 Spatial analysis: Semivariograms were fit to disease incidence data from both the Salinas  
21 2013-2014 and 2014-2015 seasons (Fig. 4). Most of the rating periods in the Salinas 2013-2014  
22 season and the first two rating periods of Salinas 2014-2015 season had no discernible spatial  
23 correlation (Table 2). Of the rating periods that had discernible spatial correlation, the average

1 range of spatial correlation was 5.9 m. Two of the rating periods were fit using the Gaussian  
2 model, four were fit using the exponential model, and none of the semivariograms had a superior  
3 fit using the spherical model.

4 The Soledad 2013 and Salinas 2013-2014 epidemics exhibited higher detectable levels of *P.*  
5 *effusa* DNA nearer to the outbreak than at greater distances (Fig. 5). Linear models regressing  
6 the natural log of the copy number on the natural log of the distance suggested a statistically  
7 significant dependence of airborne inoculum concentration on distance from the assumed source  
8 and accounted for relatively high proportions of the observed variance (Fig. 6, Table 3). Linear  
9 models fitted to untransformed distance data were also significant, but had lower  $R^2$  values,  
10 suggesting that they explained less of the data than regressions using natural log transformed  
11 distance data. Both the power-law and the exponential distribution fit our data well, with over  
12 95% of the 2500 randomly created datasets failing to reject the null hypotheses in all models  
13 (Table 4). However, the  $x_{min}$  values for the exponential models were higher than those for the  
14 power-law models (Table 4).

15

16

## DISCUSSION

17 Spore trapping in the winter periods of both the Salinas 2013-2014 and 2014-2015 seasons  
18 revealed detectable, low levels of the pathogen, even in the absence of disease at the adjacent  
19 susceptible field. With relatively few spinach plantings over the fall and winter months in the  
20 Salinas Valley, the source of this airborne inoculum remains unknown. The spores may have  
21 come from infected non-commercial spinach being grown in local gardens or from long distance  
22 dispersal from outside the region. However, the overall consistency of *P. effusa* detection would  
23 suggest that the spores likely came from a local, undetected outbreak. In other spore trapping

1 studies of aerially dispersed obligate biotrophic pathogens, detection was minimal during non-  
2 host periods (Fallacy et al. 2007). This may be due to differences in local agronomic practices,  
3 or possibly a cryptic portion of the lifecycle of *P. effusa* of which we are currently unaware.

4 While *P. effusa* was detected in both the Salinas 2013-2014 and 2014-2015 seasons, there  
5 were marked differences in the overall patterns. In the Salinas 2013-2014 season, there was a  
6 relatively low but consistent proportion of *P. effusa* detected in late November and December.  
7 While the detection seemed to level off for much of late December, overall detection began to  
8 increase again in January as the local susceptible field was infected. In the Salinas 2014-2015  
9 season, *P. effusa* levels increased steadily through mid-January and had sporadic bursts through  
10 late-January and early-February, mirroring the increase in disease incidence. Levels of *P. effusa*  
11 DNA detection at the four cardinal traps were different in 2013-2014 season versus the 2014-  
12 2015 season, and levels of *P. effusa* DNA were particularly higher in 2013-2014 on the South  
13 and East traps in mid-January onward, mirroring the increase in disease incidence and suggestive  
14 of the NW wind flow during periods of spore release.

15 Susceptible spinach fields adjacent to the spore traps in both the Salinas 2013-2014 and  
16 2014-2015 seasons were naturally infected with downy mildew. Regular scouting and  
17 monitoring of the field for disease incidence revealed increasing disease as the epidemic  
18 progressed. Logistic curve fitting analysis suggests that both epidemics closely follow a logistic  
19 curve that is typical of a polycyclic disease (Madden et al. 2007). The maximum estimated rate  
20 of disease increase was 9.23% per day in 2014 versus 3.64% in 2015. These findings seem to  
21 qualitatively match previously described temporal pattern of outbreaks of spinach downy mildew  
22 in The Netherlands (Frinking and Linders 1986), although the rate of disease increase in our  
23 study appears to be higher. This might be due to differences in weather patterns or modern

1 agronomic practices, like increased planting density and wider beds. It may also simply be due  
2 to differences in disease scouting and rating techniques, as our study monitored the incidence of  
3 infected leaves and their study focused on disease severity as area of leaf affected.

4 Understanding the scale of plant disease aggregation can help in disease prediction and  
5 control. Plant diseases typically aggregate as disease foci, localized clusters of diseased plants  
6 (Zadoks and van den Bosch 1994). This clustering occurs on different spatial scales, with  
7 smaller foci aggregating into larger foci, possibly even expanding to regional scale epidemics.  
8 We used semivariograms to assess the area of spatial dependence in our two Salinas epidemics.  
9 We found that disease was spatially dependent within an average radius of 5.9 m. This  
10 corresponds approximately to the width of three beds, a relatively small scale in terms of the  
11 total spinach acreage in a typical field. This range corresponds closely to the range of other  
12 downy mildew pathogens, including *Pseudoperonospora humuli* and *Hyaloperonospora*  
13 *brassicae*, which had average ranges of approximately 7.5 m and 5 m, respectively (Johnson et  
14 al. 1991; Stein et al. 1994). The similarity in the range might be due to similar dispersal  
15 mechanisms and infection capabilities. The results indicated that scouting to estimate disease  
16 incidence for spinach downy mildew should be based on samples separated by distances of 5.9 m  
17 to obtain individual samples that are statistically independent.

18 In spore trapping studies, spore detection rates are often tightly linked with disease incidence  
19 and severity in nearby crops (Granke et al. 2014). In the Salinas 2013-2014 season, as disease  
20 incidence increased in the susceptible crop, *P. effusa* detection increased as well. At the end of  
21 the Salinas 2014-2015 season, levels of detectable *P. effusa* were more sporadic even as the  
22 disease incidence increased. This may have been due to unsuitable weather factors for  
23 sporulation and dispersal. It is also possible that the observed increase in disease symptoms,

1 such as chlorosis and decline of leaves, may not have been accompanied by proportional  
2 amounts of increased sporulation. In some downy mildew species, symptoms and sporulation  
3 are expressed at different levels under different environmental conditions (Aegerter et al. 2003).  
4 Spore trap monitoring in both the Salinas 2013-2014 and 2014-2015 seasons showed relatively  
5 large levels of *P. effusa* DNA detection just as symptoms were first appearing in mid-January of  
6 both seasons. It is possible that this could represent sporulation during the early stages of  
7 infection, when the leaves have not yet developed chlorosis, throughout most of the field plot.  
8 This cryptic sporulation could lead to large outbreaks that may seem to appear suddenly when  
9 conditions are conducive for the development of chlorosis.

10 Oospores play a significant role in other downy mildew diseases, allowing the pathogens to  
11 persist in soil and spread on seeds (Cohen and Sackston 1974; Gaag and Frinking 1997;  
12 Garibaldi et al. 2004; Montes-Borrego et al. 2009). The recent findings of viable oospores of *P.*  
13 *effusa* affixed to spinach seeds may account for inter-regional dispersal and overwintering of the  
14 pathogen (Kunjeti et al. 2015). It is possible that due to the high number of spinach seeds used  
15 in crop establishment (approximately 10 M seeds per ha) and the large and increasing acreage of  
16 harvested spinach, even low rates of seed contamination with oospores could have significant  
17 impacts on disease incidence in aggregate (Koike et al. 2011). Due to the late onset of disease in  
18 both seasons, it is unlikely that oospores played a role in our field plots (Frinking and Linders  
19 1986). It is more likely that disease was initiated by airborne sporangia blown from unidentified  
20 local sources.

21 Early studies in aerobiology proposed that many plant pathogenic fungal and oomycete  
22 spores are exponentially distributed, allowing for long distance dispersal (LDD) (Aylor 2003;  
23 Fitt et al. 1987). LDD on continental scales has been described for several downy mildew

1 pathogens, notably *Peronospora tabacina* and *Pseudoperonospora cubensis* (LaMondia and  
2 Aylor 2001; Lucas 1980; Ojiambo and Holmes 2011; Savory et al. 2011). These two species  
3 take advantage of meteorological conditions that carry spores from the southeastern US up  
4 through eastern and central Canada, in what is referred to as the ‘*Peronospora* Pathway’ (Aylor  
5 2003). The pathogens overwinter in the warmer southern regions, and then recolonize northern  
6 regions that have experienced extirpation. It is difficult to assess if *Peronospora effusa* disperses  
7 from the Salinas Valley to the Yuma and Imperial Valleys through an analogous pathway. The  
8 *Peronospora* pathway that links the southeastern and north-central USA is typically completed  
9 by multiple regional-scale dispersal jumps, rather than a single, continental-wide dispersal event.  
10 The *Peronospora* Pathway is possible in the eastern US, where cucurbit and tobacco hosts are  
11 widespread. Spinach, in contrast, is rarely grown on a significant scale anywhere in between the  
12 widely separated Salinas and Imperial/Yuma valleys in the western US.

13 Understanding how aerial spores are distributed across space can help to improve disease  
14 management practices (Carisse et al. 2008a; Carisse et al. 2008b). In conjunction with a Salinas  
15 Valley wide trapping study (Choudhury et al. unpublished), we were able to monitor *P. effusa*  
16 levels at two active epidemics as well as sites throughout the valley. Overall, *P. effusa* levels  
17 adjacent to the epidemics were orders of magnitude higher than those further from the outbreaks.  
18 However, while detection levels decreased with distance from the epidemic, inoculum detection  
19 was fairly uniform at long distances. This ‘fat tail’ effect is typical of power law distributions  
20 (Clauset et al. 2009). We were unable to distinguish if our data better fit the power law or  
21 exponential distribution. Making this distinction is notoriously difficult because of the challenge  
22 in making sufficient numbers of observations at large distances from the source. These distant  
23 observations allow the tails of the distributions to be differentiated. The dispersal of *P. schachtii*

1 from infected sugar beet plants has been previously characterized (Fitt et al. 1987). Fitt et al.  
2 (1987) found that the exponential distribution fit their data slightly better, although the values of  
3 their parameters such as evaluation at distances up to 80 m from the source were different from  
4 our own. The authors also analyzed data from many different pathogens, and noted that smaller  
5 spores (<10  $\mu\text{m}$ ) tended to fit a power law distribution better than larger spores, such as those of  
6 *P. effusa*, whose sporangia are typically 21-33  $\mu\text{m}$  long (Choi et al. 2007).

7 This study highlights some of the complexities and difficulties in using spore traps as part of  
8 a decision support system for spinach downy mildew. However, at the Salinas plot in 2013-2014  
9 and 2014-2015, the increase in disease incidence was reflected in the increasing levels of *P.*  
10 *effusa* DNA detectable in spore traps, providing the potential opportunity to exploit trap and  
11 DNA-based detection at the field or ranch level for an early warning system on that scale. On a  
12 larger scale, long distance dispersal events could obscure the source of detected levels of *P.*  
13 *effusa* by creating a uniform blanket of spores across the region as demonstrated previously  
14 (Choudhury et al. unpublished). Epidemics occur at different speeds and with different spatial  
15 aggregations and scales. While these findings highlight some of the uncertainty in the spinach  
16 downy mildew system, they also highlight common features with other disease systems.  
17 Predicting disease outbreaks and finding practical control methods remain as critically important  
18 goals for protecting susceptible spinach crops.

19

20

#### ACKNOWLEDGMENTS

21 We thank the California Leafy Greens Research Program (CLGRP) and the California  
22 Department of Agriculture Specialty Crop Block Grant Program (Number SCB14043) for  
23 funding this research. We thank Dr. Walt Mahaffee (USDA-ARS, Corvallis, OR) for providing

1 some spore trap materials and advice, and Lorena Ochoa (USDA-ARS, Salinas, CA) and Ruben  
2 Pena (Hartnell College, Salinas, CA) for collecting spore trap samples. We thank Sharon  
3 Benzen for maintaining the Salinas USDA ARS spinach plots. We thank Leonard Montenegro  
4 and Raquel Gearheart for weather data programming and support. We also thank Kari Arnold  
5 and Dr. Christophe Gigot for helpful comments on data analysis.

6

7

### LITERATURE CITED

- 8 Aegerter, B. J., Nuñez, J. J., and Davis, R. M. 2003. Environmental factors affecting rose downy  
9 mildew and development of a forecasting model for a nursery production system. *Plant Dis.*  
10 87:732-738.
- 11 Aylor, D. E. 2003. Spread of plant disease on a continental scale: role of aerial dispersal of  
12 pathogens. *Ecology* 84:1989-1997.
- 13 Brown, J. K., and Hovmøller, M. S. 2002. Aerial dispersal of pathogens on the global and  
14 continental scales and its impact on plant disease. *Science* 297:537-541.
- 15 Byford, W. J. 1967. Host specialization of *Peronospora farinosa* on *Beta*, *Spinacia* and  
16 *Chenopodium*. *T. Brit. Mycol. Soc.* 50:603-607.
- 17 Carisse, O., Savary, S., and Willocquet, L. 2008. Spatiotemporal relationships between disease  
18 development and airborne inoculum in unmanaged and managed *Botrytis* leaf blight  
19 epidemics. *Phytopathology* 98:38-44.
- 20 Carisse, O., McRoberts, N., and Brodeur, L. 2008. Comparison of monitoring- and weather-  
21 based risk indicators of *Botrytis* leaf blight of onion and determination of action thresholds.  
22 *Can. J. Plant Pathol.* 30:442-456.

- 1 Choi, Y. J., Klosterman, S. J., Kummer, V., Voglmayr, H., Shin, H. D., and Thines, M. 2015.  
2 Multi-locus tree and species tree approaches toward resolving a complex clade of downy  
3 mildews (Straminipila, Oomycota), including pathogens of beet and spinach. *Mol.*  
4 *Phylogenet. Evol.* 86:24-34.
- 5 Choi, Y. J., Hong, S. B., and Shin, H. D. 2007. Re-consideration of *Peronospora farinosa*  
6 infecting *Spinacia oleracea* as distinct species, *Peronospora effusa*. *Mycol. Res.* 111:381-  
7 391.
- 8 Clauset, A., Shalizi, C. R., and Newman, M. E. 2009. Power-law distributions in empirical data.  
9 *SIAM Rev.* 51:661-703.
- 10 Cohen, Y., and Sackston, W. E. 1974. Seed infection and latent infection of sunflowers by  
11 *Plasmopara halstedii*. *Can. J. Bot.* 52:231-238.
- 12 Coop, L., Grove, G., Fox, A., Daly, C., Mahaffee, W., and Thomas, C. 2009. Novel delivery IPM  
13 tools in real time for decision support-pull. *Phytopathology* 99:S181.
- 14 Correll, J. C., Bluhm, B. H., Feng, C., Lamour, K., Du Toit, L. J., and Koike, S. T. 2011.  
15 Spinach: better management of downy mildew and white rust through genomics. *Eur. J.*  
16 *Plant Pathol.* 129:193-205.
- 17 Curriero, F. C., and Lele, S. 1999. A composite likelihood approach to semivariogram  
18 estimation. *J Agric. Biol. Envir. S.* 4:9-28.
- 19 Falacy, J. S., Grove, G. G., Mahaffee, W. F., Galloway, H., Glawe, D. A., Larsen, R. C., and  
20 Vandemark, G. J. 2007. Detection of *Erysiphe necator* in air samples using the polymerase  
21 chain reaction and species-specific primers. *Phytopathology* 97:1290-1297.

- 1 Feng, C., Correll, J. C., Kammeijer, K. E., and Koike, S. T. 2014. Identification of new races and  
2 deviating strains of the spinach downy mildew pathogen *Peronospora farinosa* f. sp.  
3 *spinaciae*. Plant Dis. 98:145-152.
- 4 Fitt, B. D., Todd, A. D., McCartney, H. A., and Macdonald, O. C. 1987. Spore dispersal and  
5 plant disease gradients; a comparison between two empirical models. J. Phytopathol.  
6 118:227-242.
- 7 Frinking, H. D., and Van der Stoel, M. C. 1987. Production of conidia by *Peronospora farinosa*  
8 f. sp. *spinaciae*. Neth. J. Plant Pathol. 93:189-194.
- 9 Frinking, H. D., and Linders, E. G. A. 1986. A comparison of two pathosystems: downy mildew  
10 on *Spinacia oleracea* and on *Chenopodium album*. Neth. J. Plant Pathol. 92:97-106.
- 11 Fox, A. D. 2011. MtnRT White Paper: Summary of the MtnRT System. Providing weather  
12 inputs for plant disease models. Published at [www.foxweather2.com](http://www.foxweather2.com). August 31, 2011, 45  
13 pp.
- 14 Gaag, D. V. D., and Frinking, H. D. 1997. The infection court of faba bean seedlings for  
15 oospores of *Peronospora viciae* f. sp. *fabae* in soil. J. Phytopathol. 145:257-260.
- 16 Gadoury, D. M., Cadle-Davidson, L., Wilcox, W. F., Dry, I. B., Seem, R. C., and Milgroom, M.  
17 G. 2012. Grapevine powdery mildew (*Erysiphe necator*): a fascinating system for the study  
18 of the biology, ecology and epidemiology of an obligate biotroph. Mol. Plant Pathol. 13:1-  
19 16.
- 20 Garibaldi, A., Minuto, G., Bertetti, D., and Gullino, M. L. 2004. Seed transmission of  
21 *Peronospora* sp. of basil. Z. Pflanzenkr. Pflanzenschutz 111:465-469.

- 1 Granke, L. L., Morrice, J. J., and Hausbeck, M. K. 2014. Relationships between airborne  
2 *Pseudoperonospora cubensis* sporangia, environmental conditions, and cucumber downy  
3 mildew severity. *Plant Dis.* 98:674-681.
- 4 Johnson, D. A., Alldredge, J. R., Allen, J. R., and Allwine, R. 1991. Spatial pattern of downy  
5 mildew in hop yards during severe and mild disease epidemics. *Phytopathology* 81:1369-  
6 1374.
- 7 Kellogg, C. A., and Griffin, D. W. 2006. Aerobiology and the global transport of desert dust.  
8 *Trends Ecol. Evol.* 21:638-644.
- 9 Klosterman, S. J., Anchieta, A., McRoberts, N., Koike, S. T., Subbarao, K. V., Voglmayr, H.,  
10 Choi, Y., Thines, M., and Martin F. N. 2014. Coupling spore traps and quantitative PCR  
11 assays for detection of the downy mildew pathogens of spinach (*Peronospora effusa*) and  
12 beet (*P. schachtii*). *Phytopathology* 104:1349-1359.
- 13 Koike, S. T., Cahn, M., Cantwell, M., Fennimore, S., LeStrange, M., Natwick, E., Smith, R. F.,  
14 and Takele, E. 2011. Spinach production in California. *Univ. Calif. Agric. Nat. Resour. Publ*  
15 7212.
- 16 Kunjeti, S. G., Anchieta, A., Subbarao, K., Koike, S. T., and Klosterman, S. J. 2016. Plasmolysis  
17 and vital staining reveal viable oospores of *Peronospora effusa* in spinach seed lots. *Plant*  
18 *Dis.* 100:59-65.
- 19 LaMondia, J. A., and Aylor, D. E. 2001. Epidemiology and management of a periodically  
20 introduced pathogen. *Biol. Invasions* 3:273-282.
- 21 Lucas, G. B. 1980. The war against blue mold. *Science* 210:147-153.
- 22 Madden, L. V., Hughes, G., and van den Bosch, F. 2007. *The Study of Plant Disease Epidemics.*  
23 The American Phytopathological Society, St. Paul, MN.

- 1 McDonald, B. A., and Linde, C. 2002. Pathogen population genetics, evolutionary potential, and  
2 durable resistance. *Annu. Rev. Phytopathol.* 40:349-379.
- 3 Mesinger, F., DiMego, G., Kalnay, E., Mitchell, K., Shafran, P.C., Ebisuzaki, W., Jovic, D.,  
4 Woollen, J., Rogers, E., Berbery, E. H., Ek, M.B., Fan, Y., Grumbine, R., Higgins, W., Li,  
5 H., Lin, Y., Manikin, G., Parrish, D., and Shi, W. 2006. North American Regional  
6 Reanalysis: A long-term, consistent, high-resolution climate dataset for the North American  
7 domain, as a major improvement upon the earlier global reanalysis datasets in both  
8 resolution and accuracy. *Bull. Amer. Meteor. Soc.* 87:343-360.
- 9 Montarry, J., Corbière, R., and Andrivon, D. 2007. Is there a trade-off between aggressiveness  
10 and overwinter survival in *Phytophthora infestans*? *Funct. Ecol.* 21:603-610.
- 11 Montes-Borrego, M., Landa, B. B., Navas-Cortés, J. A., Muñoz-Ledesma, F. J., and Jiménez-  
12 Díaz, R. M. 2009. Role of oospores as primary inoculum for epidemics of downy mildew  
13 caused by *Peronospora arborescens* in opium poppy crops in Spain. *Plant Pathol.* 58:1092-  
14 1103.
- 15 Mouen Bedimo, J. A., Bieysse, D., Cilas, C., and Nottéghem, J. L. 2007. Spatio-temporal  
16 dynamics of arabica coffee berry disease caused by *Colletotrichum kahawae* on a plot scale.  
17 *Plant Dis.* 91:1229-1236.
- 18 Ojiambo, P. S., and Holmes, G. J. 2011. Spatiotemporal spread of cucurbit downy mildew in the  
19 eastern United States. *Phytopathology* 101:451-461.
- 20 Savory, E. A., Granke, L. L., Quesada-Ocampo, L. M., Varbanova, M., Hausbeck, M. K., and  
21 Day, B. 2011. The cucurbit downy mildew pathogen *Pseudoperonospora cubensis*. *Mol.*  
22 *Plant Pathol.* 12:217-226.

1 Spanu, P. D. 2012. The genomics of obligate (and nonobligate) biotrophs. *Annu. Rev.*  
2 *Phytopathol.* 50:91-109.

3 Stein, A., Kocks, C. G., Zadoks, J. C., Frinking, H. D., Ruissen, M. A., and Myers, D. E. 1994. A  
4 geostatistical analysis of the spatio-temporal development of downy mildew epidemics in  
5 cabbage. *Phytopathology* 84:1227-1239.

6 Thiessen, L. D., Keune, J. A., Neill, T. M., Turechek, W. W., Grove, G. G., and Mahaffee, W. F.  
7 2016. Development of a grower-conducted inoculum detection assay for management of  
8 grape powdery mildew. *Plant Pathol.* 65:238-249.

9 Thines, M., and Choi, Y.-J. 2016. Evolution, diversity, and taxonomy of the Peronosporaceae,  
10 with focus on the genus *Peronospora*. *Phytopathology* 106:6-18.

11 Van den Bosch, F., Frinking, H. D., Metz, J. A. J., and Zadoks, J. C. 1988. Focus expansion in  
12 plant disease. III: Two experimental examples. *Phytopathology* 78:919-925.

13 Wu, B. M., Van Bruggen, A. H. C., Subbarao, K. V., and Pennings, G. G. H. 2001. Spatial  
14 analysis of lettuce downy mildew using geostatistics and geographic information systems.  
15 *Phytopathology* 91:134-142.

16 Zadoks, J. C., and Van den Bosch, F. 1994. On the spread of plant disease: a theory on foci.  
17 *Annu. Rev. Phytopathol.* 32:503-521.

18  
19  
20  
21  
22  
23

1 TABLE 1. Parameters from the logistic growth model for spinach downy mildew epidemics in  
2 the Salinas site in 2013-2014 and 2014-2015, as illustrated in Fig. 1

3

Year	K	$\beta$	r	Slope	AUDPC	R <sup>2</sup>	RSS
2013-2014	78.1	21.57	0.475	9.23	3019.3	0.999	0.637
2014-2015	51.8	10.25	0.282	3.64	1282.9	0.994	1.709

4  
5  
6  
7  
8  
9  
10  
11  
12  
13  
14  
15  
16  
17  
18  
19  
20  
21  
22

1 TABLE 2. Parameters from the semivariograms describing spatial patterns of spinach downy  
 2 mildew disease incidence at the Salinas site during epidemics in 2013-2014 and 2014-2015

3

Year	Rating Period	Range	Sill	C/Co+C	MLCL <sup>a</sup>	RSS	R <sup>2</sup>	Model
2013/4	1,2	...	...	0.00	...	...	...	Pure nugget effect
2013/4	3	5.40	429.2	1.00	-22734.5	346360.7	0.040	Exponential
2013/4	4,5	...	...	0.00	...	...	...	Pure nugget effect
2014/5	1,2	...	...	0.00	...	...	...	Pure nugget effect
2014/5	3	5.75	22.3	1.00	-61077.7	582.7	0.118	Exponential
2014/5	4	6.79	20.2	0.17	-60076.8	429.7	0.165	Gaussian
2014/5	5	2.70	298.1	0.52	-87851.2	18000.2	0.217	Gaussian
2014/5	6	4.24	489.9	1.00	-92951.1	58676.0	0.295	Exponential
2014/5	7	10.39	484.4	0.54	-92782.2	96134.8	0.299	Exponential

4 <sup>a</sup> Maximum log-composite-likelihood.

5

6

7

8

9

10

11

12

13

14

15

16

17

18

1 TABLE 3. Results from the linear regression of the natural log of *Peronospora effusa* spore trap  
2 data at different distances from epidemics in Salinas and Soledad, California, as illustrated in  
3 Fig. 6

4

Distance	Site	Intercept	Slope	R <sup>2</sup>	p-value
Natural Log	Salinas	12.05	-2.118	0.5926	1.08e-14
Natural Log	Soledad	10.57	-1.127	0.2598	5.96e-09
Untransformed	Salinas	9.92	-0.104	0.3389	1.55e-07
Untransformed	Soledad	9.64	-0.092	0.1849	1.62e-06

5  
6  
7  
8  
9  
10  
11  
12  
13  
14  
15  
16  
17  
18  
19  
20  
21  
22

1 TABLE 4. Parameters for the distribution fit for *Peronospora effusa* spore trap data from the  
 2 epidemic sites

3

Site	Model	$x_{\min}$	$\alpha$	$\lambda$	Goodness of Fit (%) <sup>a</sup>
Soledad, CA	Power-law	1945.1	1.53	...	96.6
	Exponential	246283	...	5.61e-07	99.2
Salinas, CA	Power-law	100.1	1.29	...	98.5
	Exponential	104272.2	...	6.75e-07	98.8

4

<sup>a</sup> Percent of 2500 randomly created datasets that were not significantly different from the experimental dataset.

5

6

7

8

9

10

11

12

13

14

15

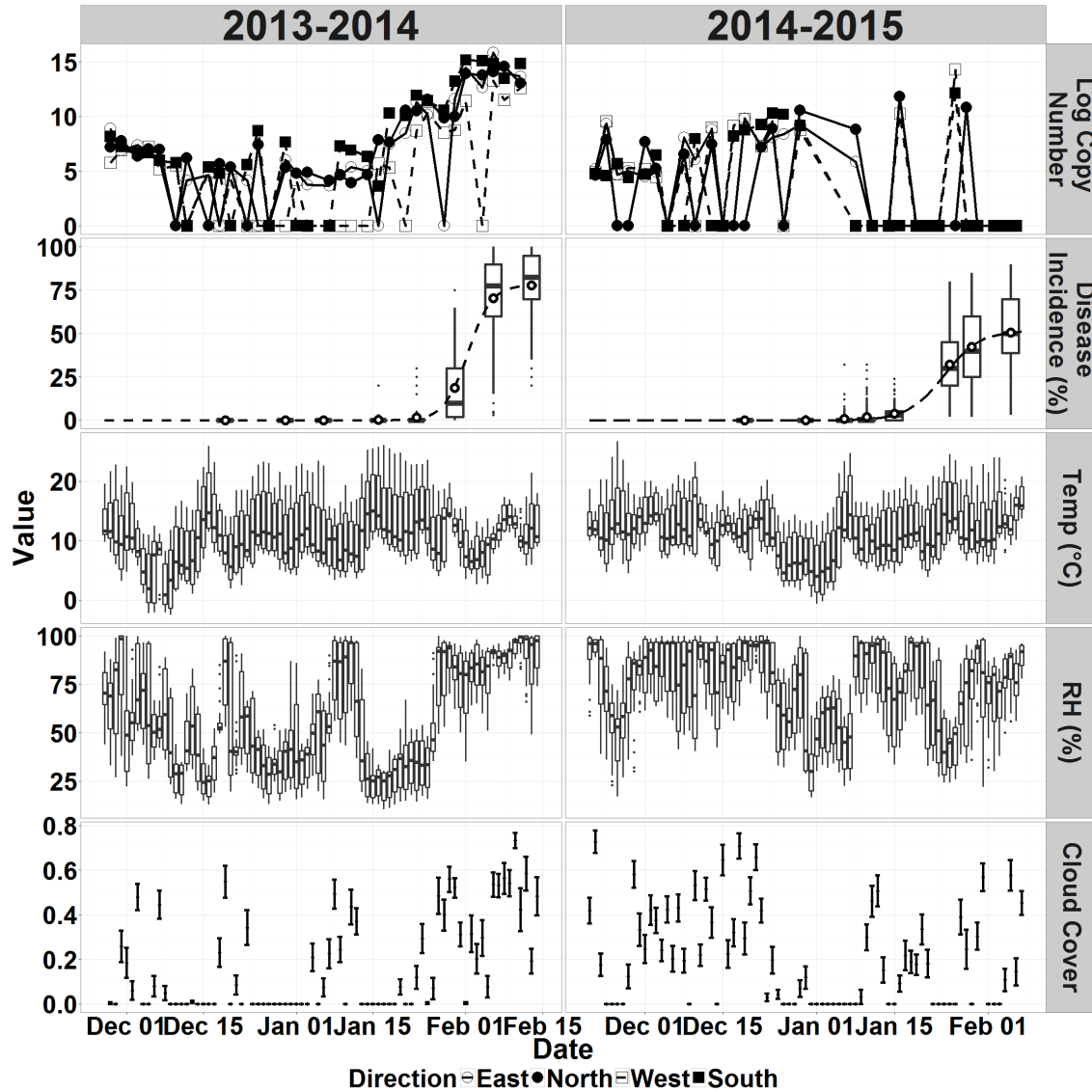
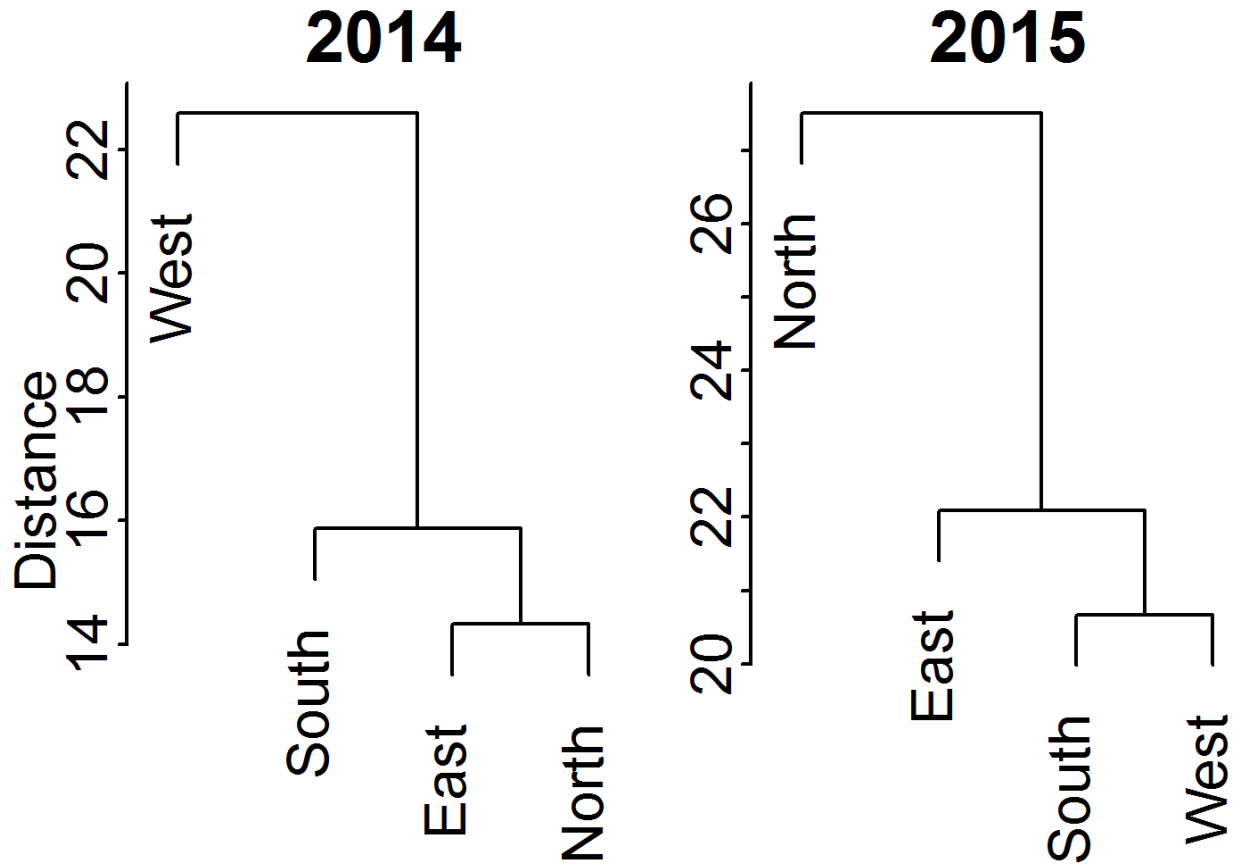
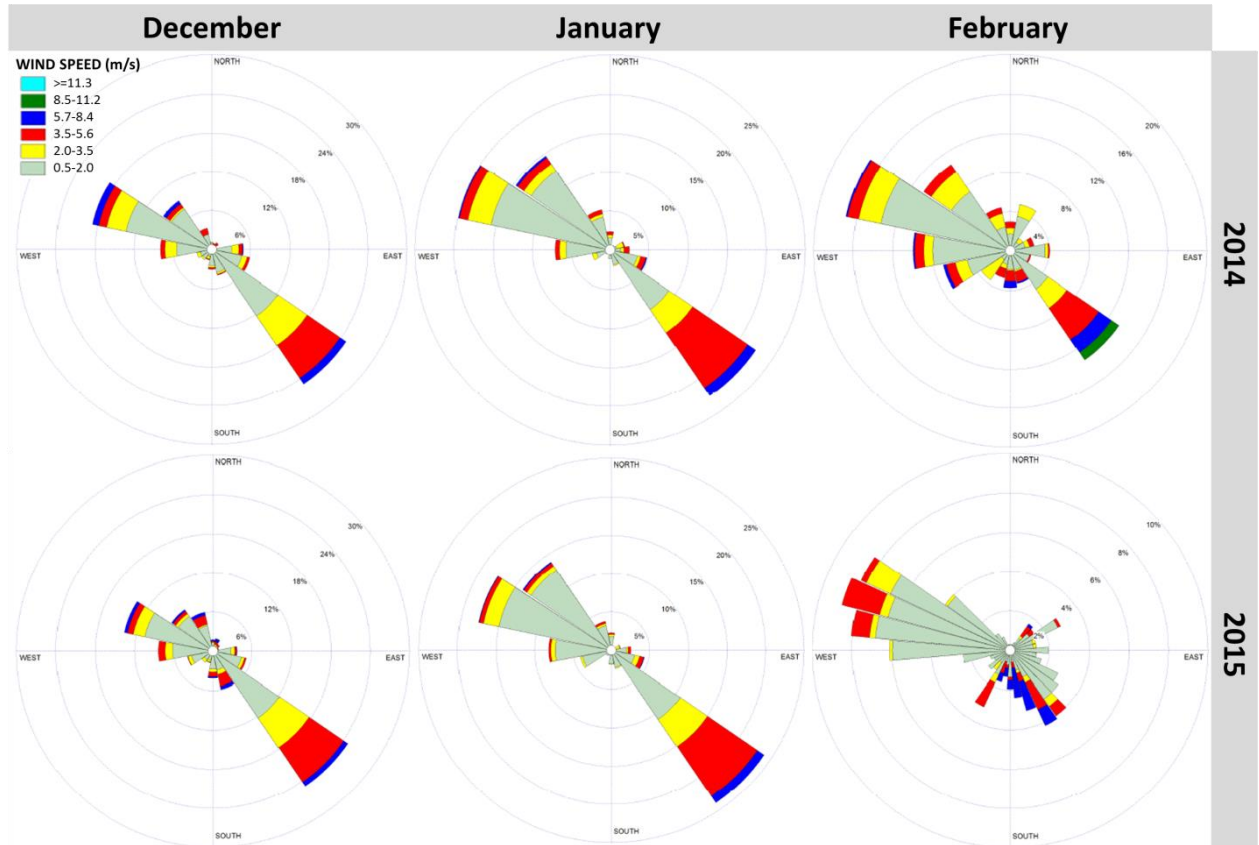


**Fig. 1.** Line plot of the natural log of *Peronospora effusa* DNA copy number from four different traps, and boxplots of disease incidence (%), temperature (°C), relative humidity (%), and mean and standard error of cloud cover during the Salinas epidemics in 2013-2014 and 2014-2015. Temperature, relative humidity, and cloud cover represent hourly data. Dashed lines in disease incidence represent results of the fitted logistic growth model of the average spinach downy mildew disease incidence, represented by hollow white circles. Parameters for the logistic growth models are given in Table 1.



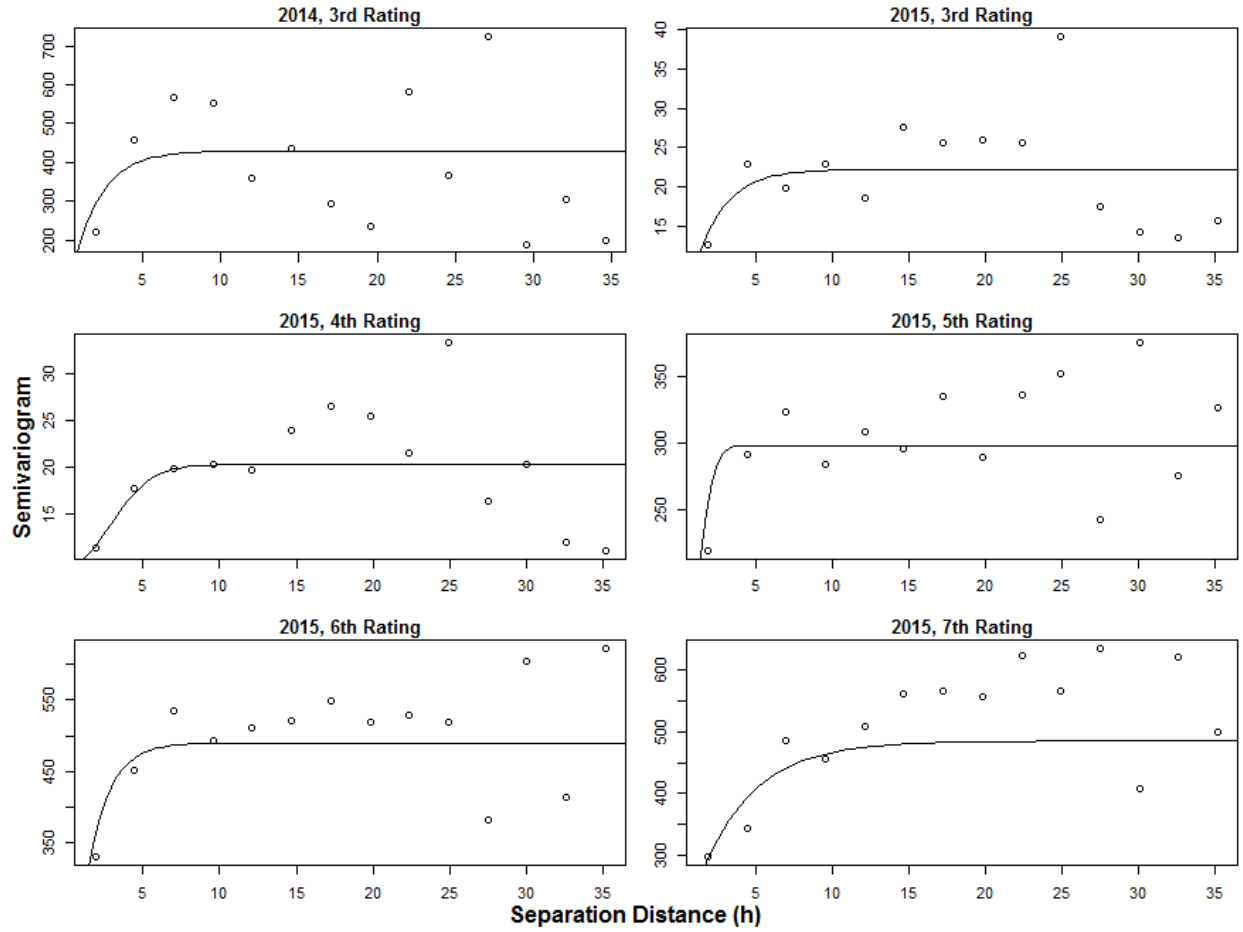
1  
2  
3  
4  
5  
6  
7  
8  
9  
10  
11  
12

**Fig. 2.** Hierarchical clustering of *Peronospora effusa* DNA copy numbers detected by qPCR from the four cardinal spore traps for the Salinas 2013-2014 and 2014-2015 winter seasons.



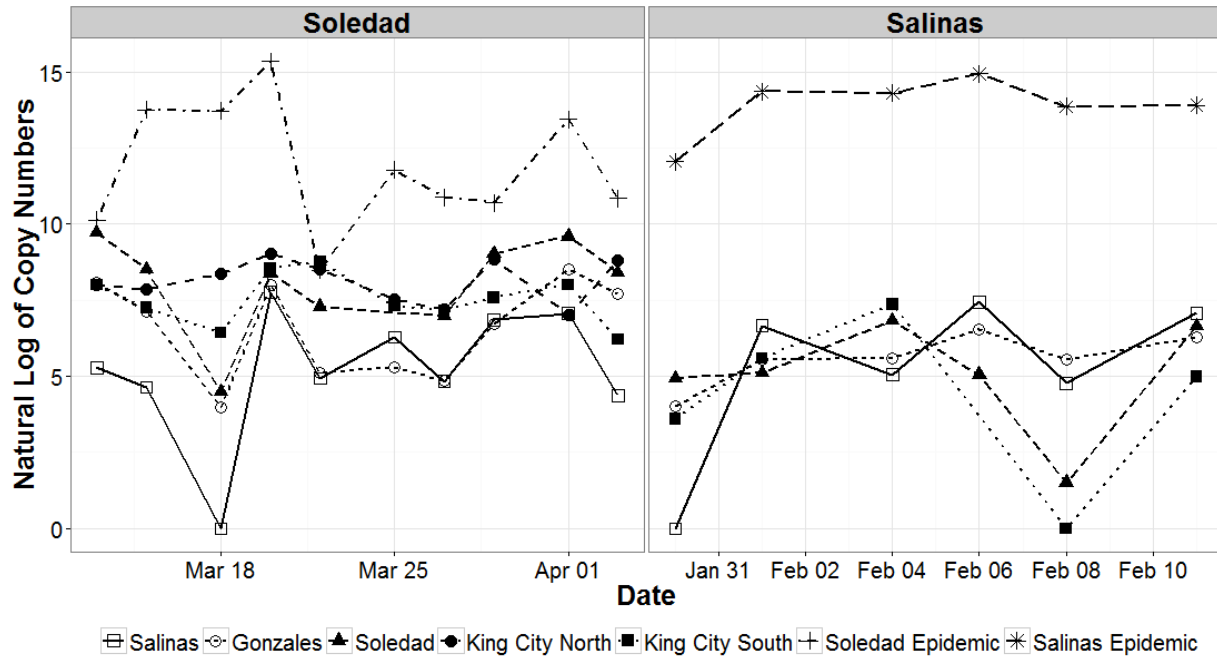
1  
 2 **Fig. 3.** Windroses illustrating wind direction and speed at the USDA ARS station in Salinas, CA  
 3 from the Salinas 2013-2014 and Salinas 2014-2015 winter seasons.

4  
 5  
 6  
 7  
 8  
 9  
 10  
 11  
 12



1  
2 **Fig. 4.** Semivariograms from different spinach downy mildew disease incidence rating periods  
3 during the Salinas epidemics in 2013-2014 and 2014-2015.

4  
5



1

2

**Fig. 5.** Daily average *Peronospora effusa* DNA copy numbers from near an epidemic and other sites throughout the Salinas Valley.

3

4

5

6

7

8

9

10

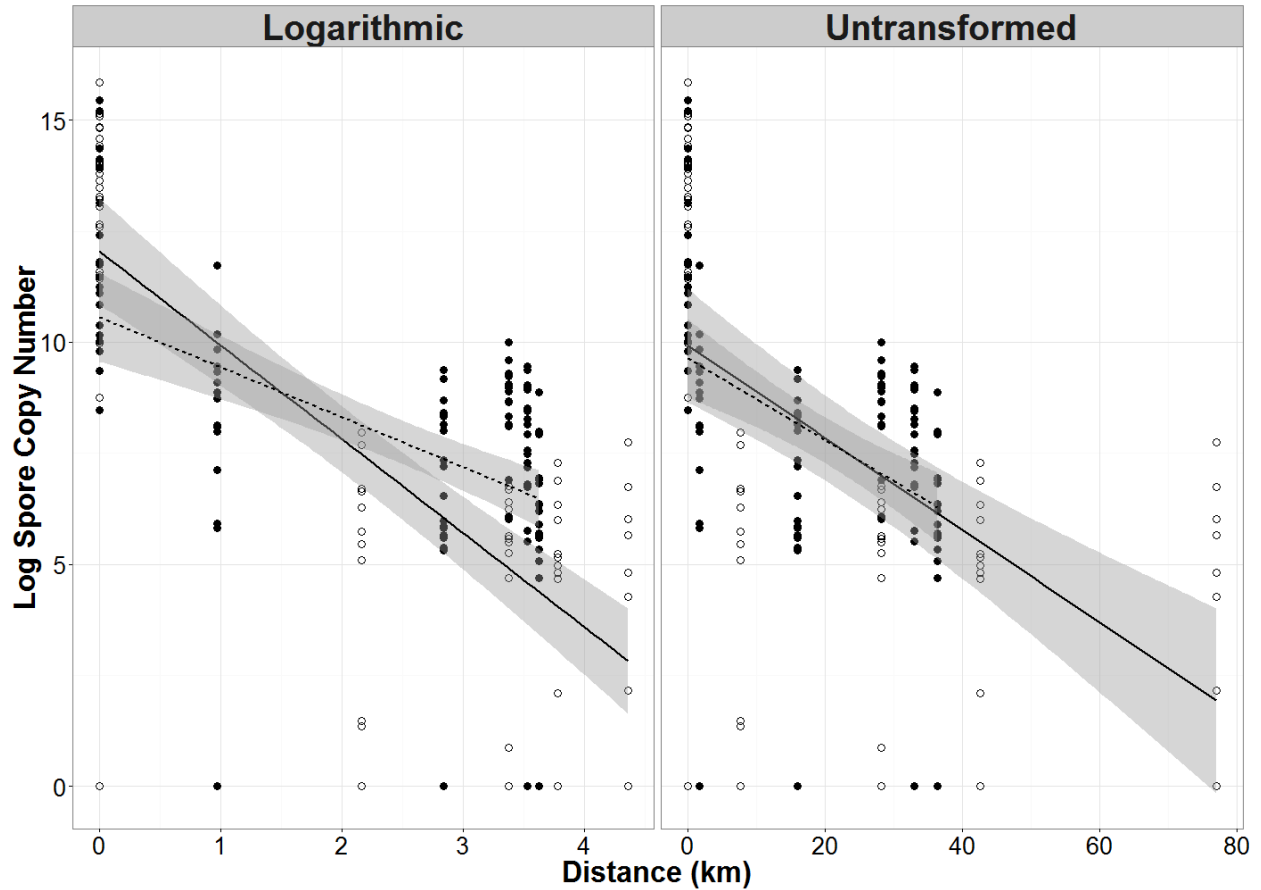
11

12

13

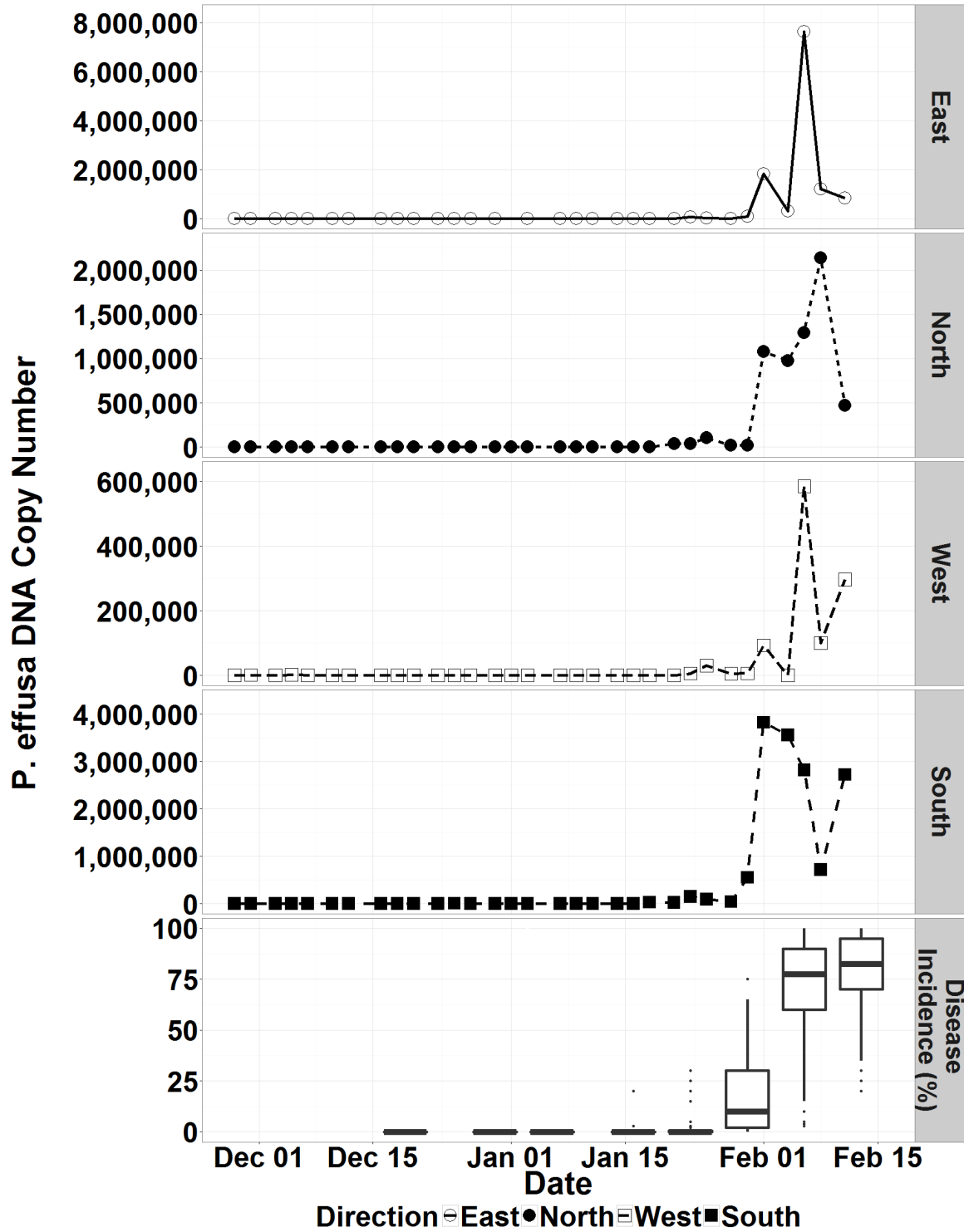
14

15

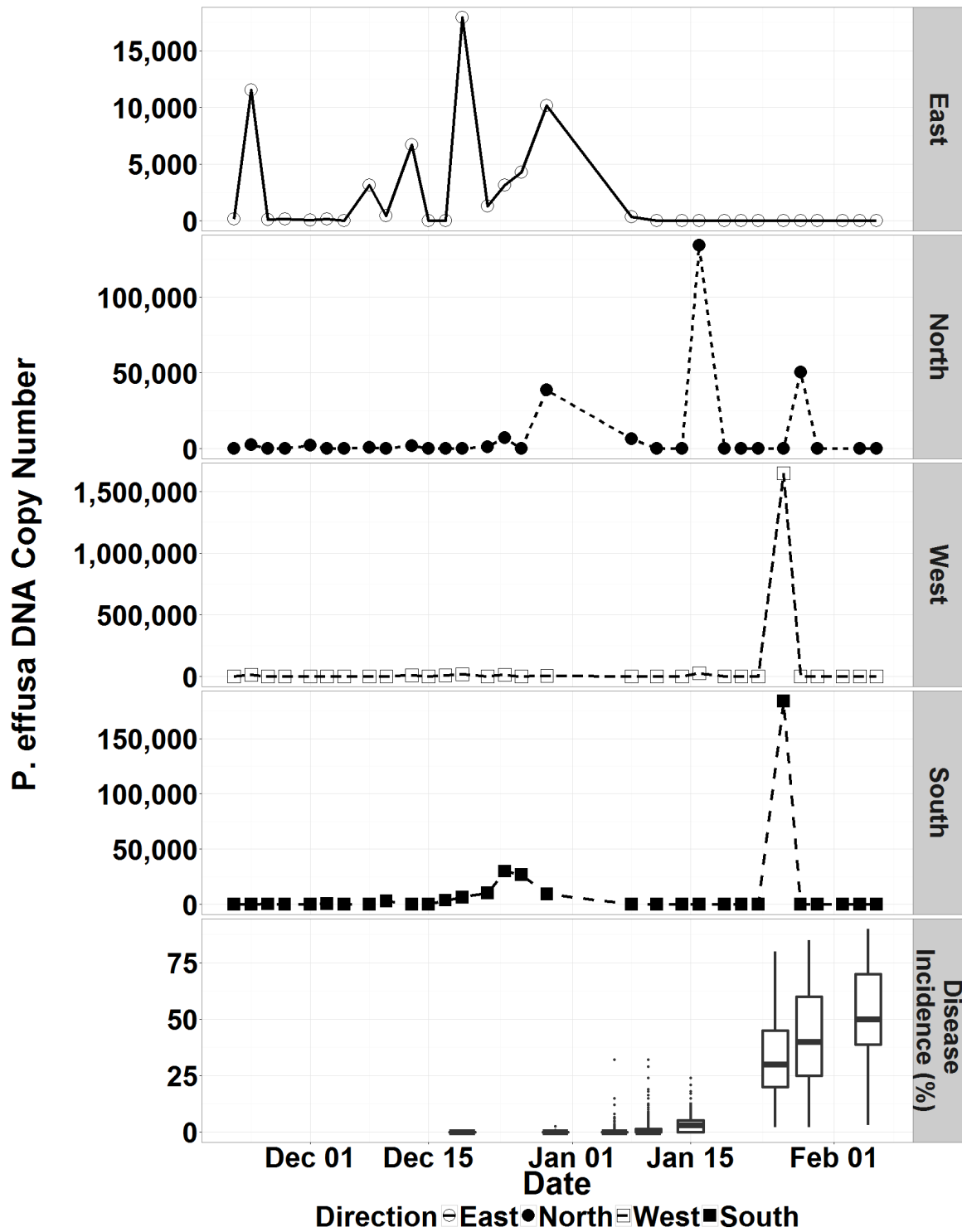


1  
 2 **Fig. 6.** Natural log of *P. effusa* DNA copy number derived from qPCR on spore traps samples  
 3 collected at an active spinach downy mildew epidemic site and from spore traps at more distant  
 4 locations. Spore trap data is plotted against both natural log and untransformed distance data.  
 5 Hollow points and solid points represent epidemics in Soledad and Salinas, California,  
 6 respectively. The dashed and solid lines represent the lines of best fit for the Soledad and Salinas  
 7 epidemics, respectively, and the gray area represents the 95% confidence interval region.  
 8 Summaries of the linear regression models are given in Table 3.

9  
 10  
 11  
 12



1  
 2 **Fig. S1.** DNA copy numbers of *Peronospora effusa* from the Salinas 2013-2014 epidemic field  
 3 site at the four cardinal spore traps. Note different scales for trap graphs.



1  
 2 **Fig. S2.** DNA copy numbers of *Peronospora effusa* from the Salinas 2014-2015 epidemic field  
 3 site at the four cardinal spore traps. Note different scales for trap graphs.